IRSTI 29.19.31

Formation of zinc selenite nanostructures in SiO_2/Si track templates with the use of two kinds of electrolytes

A.D. Akylbekova, G.G. Sarsekhan, Z.K. Baimukhanov, A.K. Dauletbekova, G.M. Aralbayeva

L.N.Gumilyov Eurasian National University, Astana, Kazakhstan
E-mail: (aiman88_88@mail.ru)

Abstract. *This paper presents studies of zinc selenite nanocrystals obtained by chemical and electrochemical deposition of zinc in a silicon dioxide track template. With the use of two kinds of electrolytes, zinc selenite nanocrystals were prepared by template synthesis and their morphological, structural and photoluminescent properties were investigated. The electrochemical deposition method was shown to be more optimal to create this crystal in comparison to the chemical deposition method. The cell parameters created by us match up with the results of other authors. Photoluminescence spectra were recorded in the spectrum interval from 2 to 4 eV at room temperature at an excitation wavelength of ~ 4 eV.*
Keywords: *silicon dioxide, chemical and electrochemical deposition, photoluminescence, zinc selenite nanocrystals.*

DOI: https://doi.org/10.32523/2616-6836-2023-145-4-6-16

1. Introduction

Zinc oxide-based materials can be commonly used in the development of luminescent and laser screens, as well as in infra-red technology. In different fields of engineering and science, scintillation sensors are required for the detection and recording of radiation. Creation of nanostructured material such zinc selenite - $ZnSeO_3$ is a smart way to explore and improve the properties of ZnO and ZnSe together instead of using them individually.

One of the prospective and intensively developing directions in modern science and technology is the establishing of technologies for the creation of nanostructured materials with specified properties, their exhaustive characterization and practical use [1]. There are many methods for obtaining nanoparticles, ranging from lithographic methods to chemical methods. Among them is the template synthesis method, which was used by us in obtaining nanocrystals is another commonly used method.

In this paper, the fast heavy ion track technology is used, which is related to the development of narrow and extended regions of radiation damage ("latent ion tracks") in different materials (especially in a silicon oxide layer) as a result of exposure to high-energy ions. [2-5]. SiO_2, widely used in semiconductor technology, was used as templates for the synthesis of nanowires and nanotubes. The etched-out pores can be infilled with different materials by chemical or

electrochemical deposition techniques. Different complexes of nanocrystals of CdTe, CdO and other wide -gap semiconductor oxides such as ZnO were safely generated by this technology in SiO_2/Si ion track templates. Such structures built on silicon substrates can be easily integrated into silicon technology. The aim of this work is to obtain $ZnSeO_3$ nanostructures by chemical and electrochemical deposition in a-SiO_2/Si-n track templates.

As new perspective materials for opto-electronics, nano-electronics and sensors are being developed, zinc selenite received in SiO_2/Si templates are of unquestioned interest. The synthesis of zinc- and selenium-based oxide semiconductor nanocrystals in SiO_2/Si track templates is undoubtedly novel. This paper is one of the first practice to demonstrate the possibility of their synthesis in SiO_2/Si matrices by chemical (CD) and electrochemical deposition (ECD) methods using two different types of electrolyte.

2. Materials and methods

The SiO_2/Si structures we used for the experiment have been described in [6-8]. The matrix synthesis was performed according to the method of templating synthesis with the use of two kinds of electrolytes. Synthesis methods are described in [9-11], where synthesis modes are described in detail. In our case, new complex crystals based on zinc selenide (ternary compounds) on zinc electrodes at voltages from 1 to 2 V were produced by template-based synthesis.

The morphology of the structures was determined by JSM7500F scanning electron microscopy (SEM). SEM analysis after etching and deposition of the obtained structures helps to control the magnitude (size), shape of nanopores and the degree of nanopore filling.

The crystallographic parameters was investigated by X-ray diffraction (XRD). XRD patterns were obtained using the X-ray diffractometer D8 ADVANCE ECO with Cu-anode comprised between angles of 2θ 30°.

Photoluminescence spectra were recorded at room temperature using an Agilent Technologies spectrofluorimeter (Cary Eclipse Fluorescence Spectrophotometer) in the spectrum interval of 300 to 800 nm at room temperature at an excitation wavelength of 300 nm.

Non-empirical calculations of the $ZnSeO_3$ crystal in the approximation of linear combinations of atomic orbitals (LCAO) were performed using the exchange–correlation functional within general gradient approximation (GGA). The calculations were performed in the CRYSTAL program.

3. Results and discussion

SEM image analyses demonstrated that major part of the nanopores of the template were filled out after CD for 30 minutes (the filling degree was 89.5%), and after CD for 15 minutes the filling level of nanopores was 39.2%, respectively. As the deposition time increases, the precipitate bulging from the nanopores on the surface was vividly presented (Fig. 1).

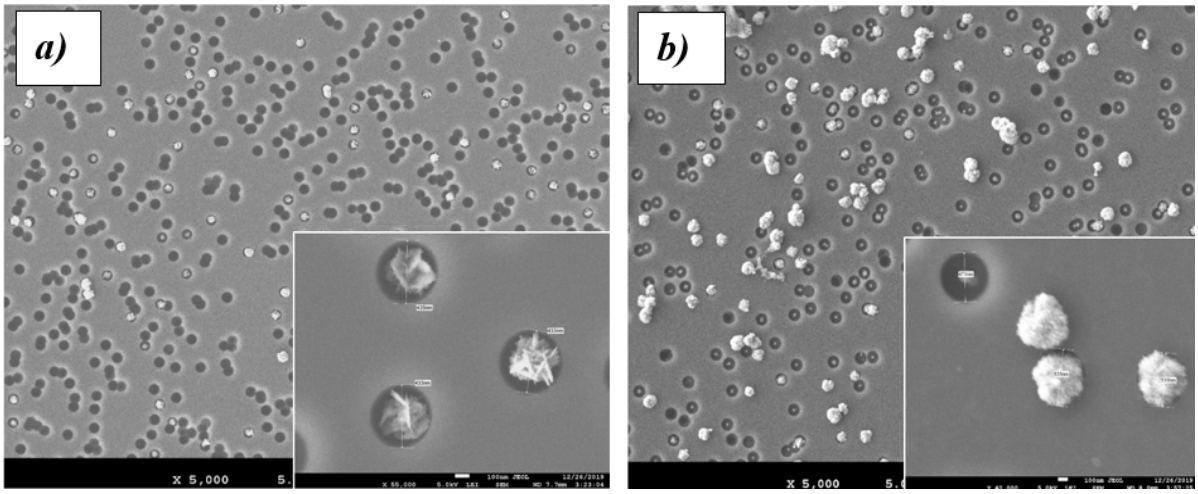

Figure 1. SEM images of nanopore filling after 15 min CD *(a)* and 30 min CD *(b).* D = 435 to 535 nm

The X-ray diffraction diagrams of the samples after chemical deposition are illustrated in fig. 2. The relevant crystallographic parameters of nanoprecipitates in ion track templates calculated from the XRD diffraction analysis data are given in Table 2. The JCPDS-78-0446 template was taken to identify the X-ray peak of orthorhombic $ZnSeO_3$.

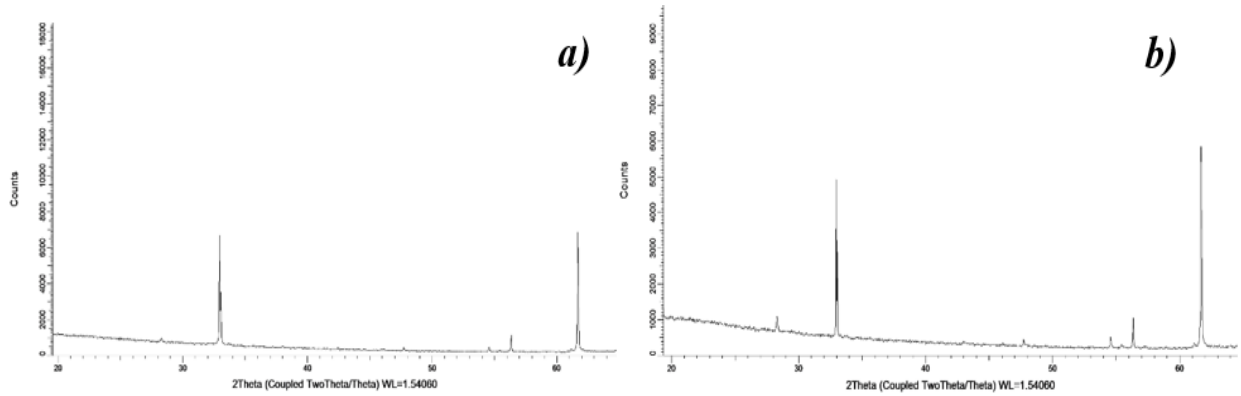

Figure 2. X-ray images of templates with nanocrystals formed by chemical precipitation: the deposition time was 15 min *(a)* and 30 min *(b).*

Table 1. Crystallographic data of $ZnSeO_3$ nanocrystals in SiO_2/Si matrices calculated from XRD data.

After CD t = 15 min									
Type of structure	Space group	hkl	2θº	Interplanar distance, Å	Crystallite size, nm	FWHM	Cell parameter, Å	Phase content, %	V, Å^3
Orthorhombic	*Pnma* (62)	121	33.831	2.72577	142.46	0.065	a=5.96223, b=7.62036, c=5.09252	100	231.38
		040	47.717	1.90441	102.31	0.094			
		321	54.535	1.68133	91.91	0.108			
		103	56.301	1.63271	138.59	0.072			
		123	61.713	1.50188	102.01	0.101			

After CD t = 30 min									
Orthor-hombic	*Pnma* (62)	200 121 040 321 103 123	28.330 32.945 47.756 54.535 56.358 61.656	3.14770 2.71660 1.90295 1.68133 1.63120 1.50313	62.05 90.40 94.51 135.67 148.88 96.47	0.147 0.102 0.102 0.073 0.067 0.107	a=5.94116, b=7.61138, c=5.09249	100	230.28

XRD data analysis for samples produced by the CD method showed the formation of $ZnSeO_3$ nanocrystals with orthorhombic crystal structure and *Pnma* space group.

Figure 3 shows SEM images of the surface after ECD. It can be seen that the degree of pore filling was significantly better compared to the samples obtained by chemical deposition. Thus, the degree of pore filling was just 88% when precipitation of precipitate was carried out at 1 V, at 1.5 V the nanopore filling degree was 90%, at 1.75 V it was 96%, and at 2 V it was 98%. It follows that, with increasing voltage, sufficient filling of nanopores is observed.

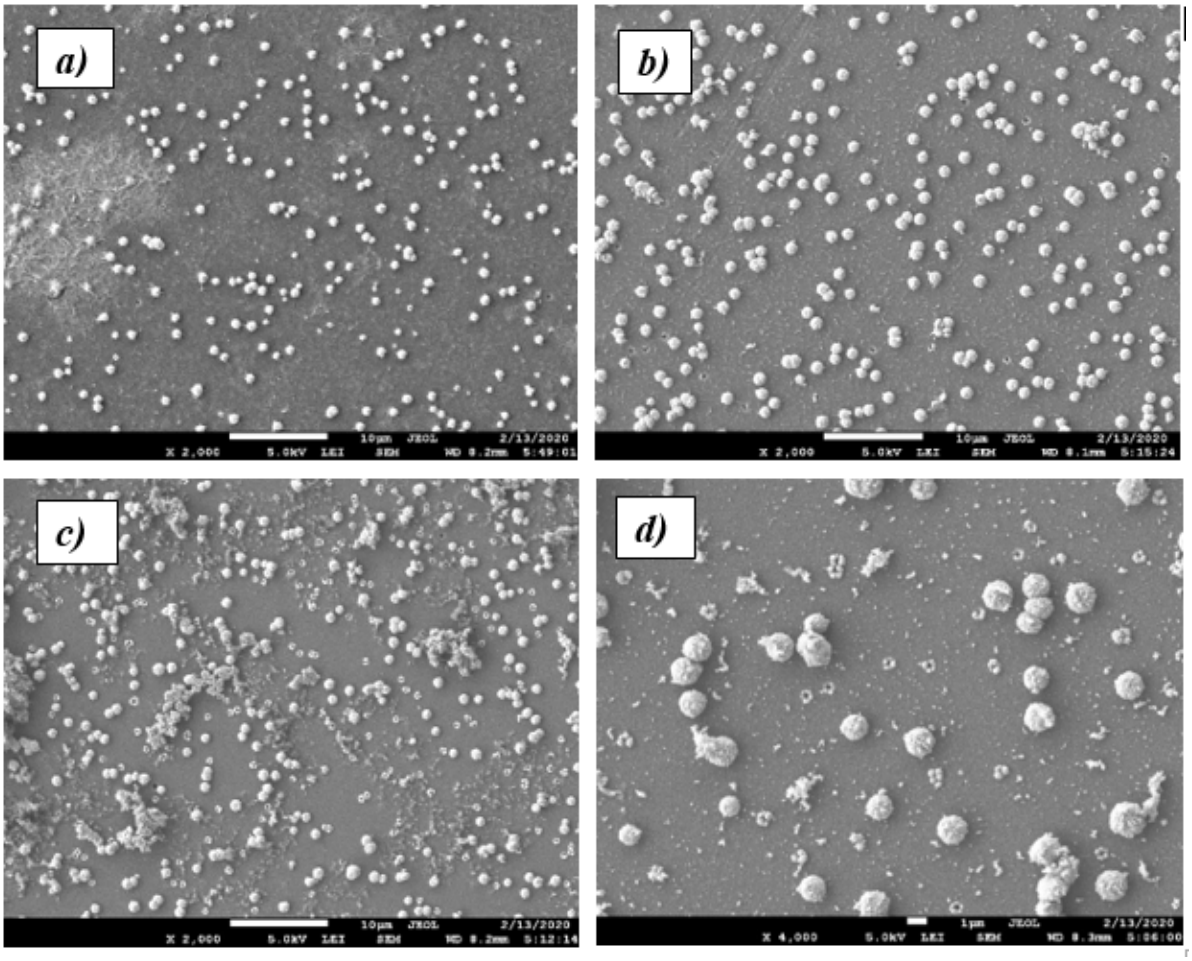

Figure 3. SEM images of nanopores after ECD at different voltages:
a) U = 1 V, *b)* U = 1.5 V, *c)* U = 1.75 V and *d)* U = 2 V. D=300 nm.

Figure 4 demonstrates the diffractograms after ECD and the results of XRD analysis are summarised in Table 2.

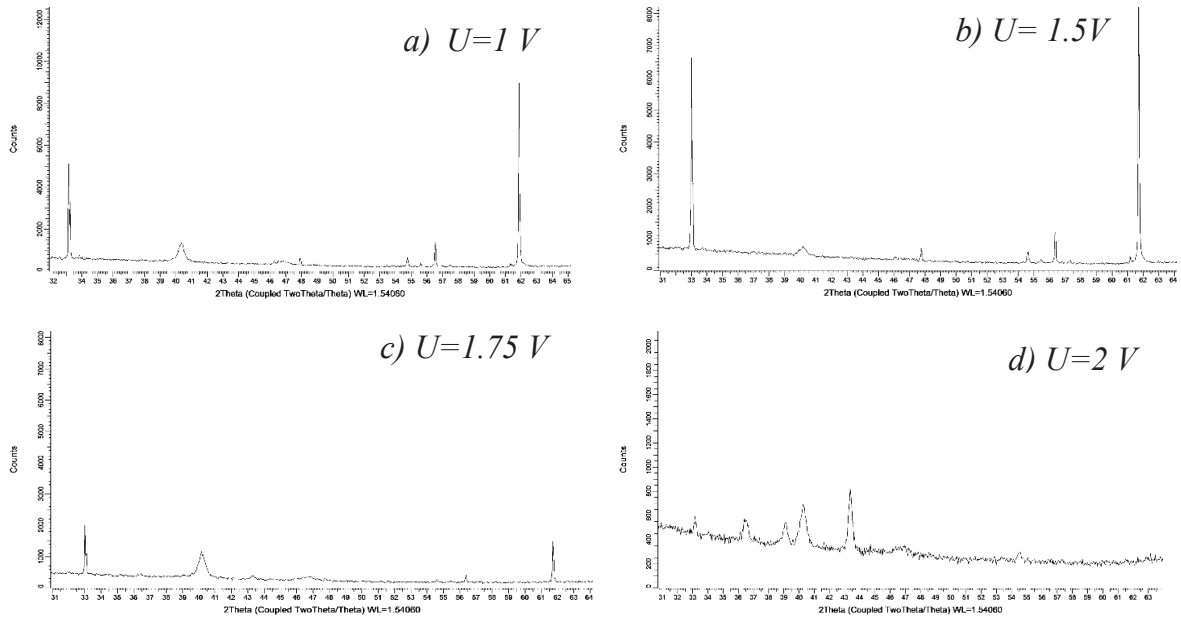

Figure 4. X-ray diffractograms of the studied samples

Figure 4 shows the diffractograms after ECD of 1V (*a*), 1.5V (*b*), 1.75V (*c*) and 2V (*d*). Thus, the generated $ZnSeO_3$ nanocrystals within the nanopores are related to the orthorhombic structure with *Pnma* space group. The cell parameters created by us match up with the results of other authors [12].

Table 2. Crystallographic data of $ZnSeO_3$ nanostructures in SiO_2/Si templates calculated from X-ray diffraction analysis data at different voltages on the electrodes.

After ECD U = 1 V									
Type of structure	Space group	hkl	2θº	Interplanar distance, Å	Crystallite size, nm	FWHM	Cell parameter, Å	Phase content, %	V, Å^3
Orthorhombic	*Pnma* (62)	121 112 123	33.092 40.275 61.747	2.70487 2.23744 1.50114	57.85 28.77 87.86	0.159 0.327 0.117	a=5.87290 b=7.71015 c=5.08066	100	230.06

After ECD U = 1.5 V									
Type of structure	Space group	hkl	2θº	Interplanar distance, Å	Crystallite size, nm	FWHM	Cell parameter, Å	Phase content, %	V, Å^3
Orthorhombic	*Pnma* (62)	121 112 202 013 103 123	32.933 40.155 47.737 54.603 56.389 61.707	2.71754 2.24380 1.90368 1.67941 1.63038 1.50201	119.81 20.53 150.16 84.24 96.23 140.29	0.077 0.458 0.064 0.118 0.104 0.073	a=5.80623, b=7.73432, c=5.09062	100	228.61

After ECD U = 1.75 V

Type of structure	Space group	hkl	2θº	Interplanar distance, Å	Crystallite size, nm	FWHM	Cell parameter, Å	Phase content, %	V, Å^3
Orthorhombic	*Pnma* (62)	121 112 123	33.131 40,.355 61.787	2.70172 2.23322 1.50027	60.25 23.73 89.53	0.153 0.396 0.115	a=5.75728, b=7.74494, c=5.08763	100	226.86

After ECD U = 2 V

Type of structure	Space group	hkl	2θº	Interplanar distance, Å	Crystallite size, nm	FWHM	Cell parameter, Å	Phase content, %	V, Å^3
Orthorhombic	*Pnma* (62)	121 112	33.131 40.156	2.70172 2.24380	76.41 18.82	0.121 0.499	a=5.78776 b=7.76468 c=5.10659	100	229.49

3.1 Photoluminescence

At room temperature, the luminescence spectra of $ZnSeO_3/SiO_2/Si$ presents a broad band between 2 eV - 3.1 eV, like in the instance of $ZnSe_2O_5/SiO_2/Si$ after deposition [13]. The photoluminescence of zinc selenite, as well as zinc diselenide, can be expected as a combination of zinc oxide and zinc selenide luminescence.

Similar to ZnO [14], the luminescence spectrum contains luminescence subbands of zinc vacancies (V_{Zn}) and oxygen vacancies (V_O). The observed bands in the photoluminescence spectrum in the 2.72 eV region are similar to the luminescence band observed in ZnSe. The bulk emission of ZnSe at the near band edge corresponds to the strong emission band at 2.84 eV. This band is according to the authors of [15] to a complex centre consisting of a zinc vacancy and an impurity small donor: $V_{Zn} + D$. As follows from figure 5, the luminescence spectrum is quite multifaceted and includes several components. Likewise, though not so complex spectra are similarly monitored in ZnO [14,16] and ZnSe [15,17]. The absence of FL with a maximum at 3.52 eV in ZnO WS is explained by exciton luminescence (3.22 eV) [18].

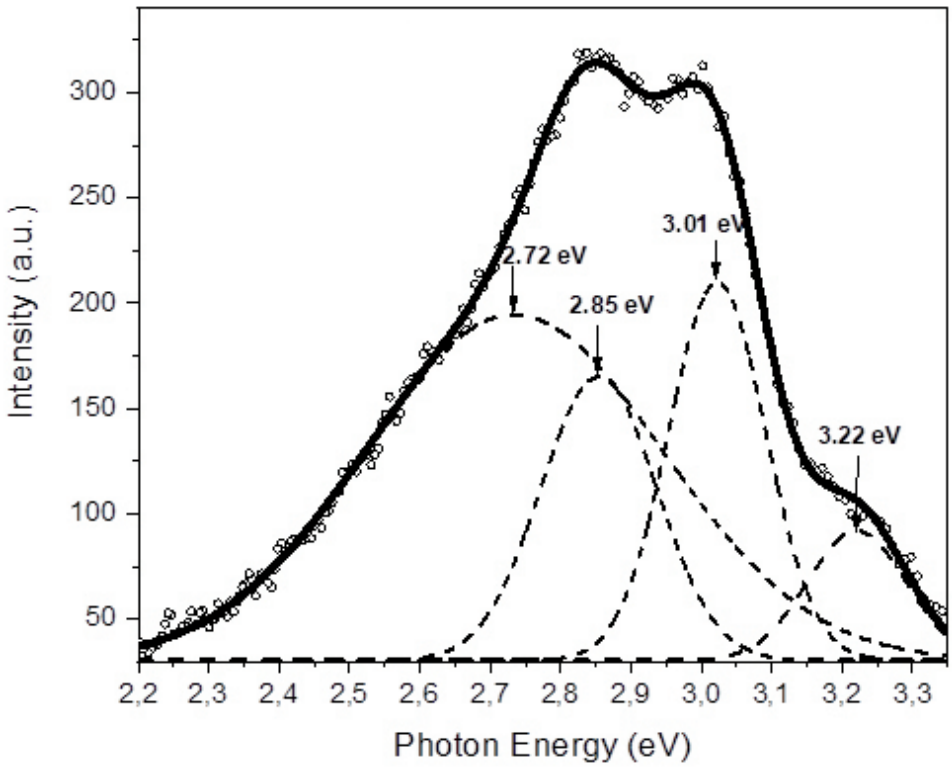

Figure 5 – Decomposition of FL spectra of zinc selenite after deposition with Gaussian curves

4. Computer modelling of $ZnSeO_3$

To confirm the obtained experimental properties of $ZnSeO_3$ nanostructures, we performed non-empirical calculations in the approximation of linear combinations of atomic orbitals (LCAO) using the LDA-PZ exchange-correlation functional of density functional theory [19, 20]. The calculations were performed in the CRYSTAL programme [21]. This programme performs calculations of the electronic structure of crystalline systems using the Hartree-Fock method, density functional theory (DFT) methods and various hybrid approximations combined with a basis (set) of local Gaussian functions for periodic (3D, 2D, 1D) systems. The programme has proved to be a reliable tool for describing different properties of a wide range of semiconductor and dielectric materials. To describe the atomic orbitals of different atoms included in the $ZnSeO_3$ crystal, the following basis sets of Gaussian-type functions were chosen: for the zinc (Zn) and oxygen (O) atom, the Jaffe basis was used [22], and for the selenium (Se) atom, the Towler basis was used [23]. To better describe both structural and electronic properties, the last *sp*-orbital of the original Se was removed. The effective atomic charges and bond occupancies were calculated using the Malliken analysis [24].

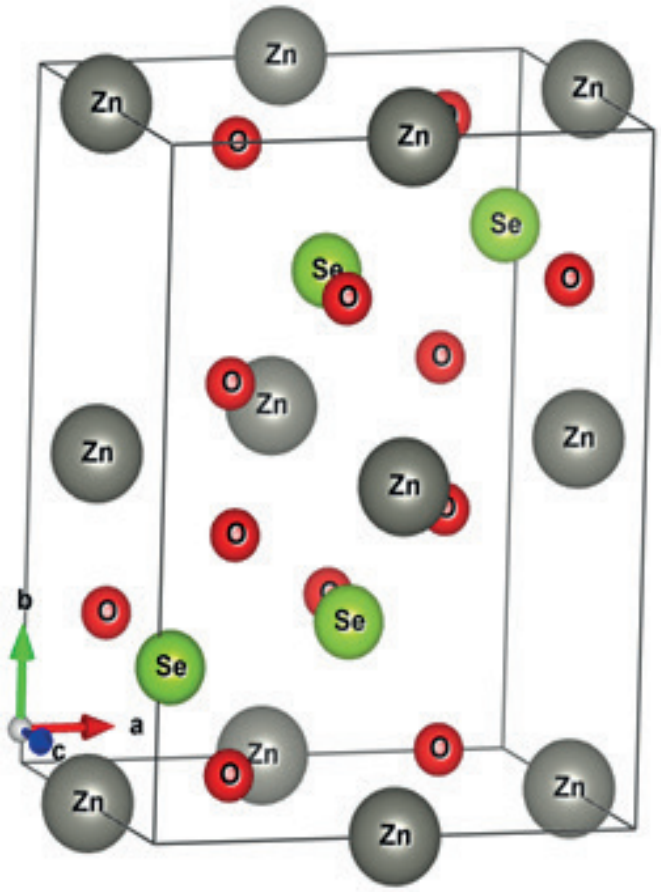

Figure 6 - Atomic structure of the unit cell of $ZnSeO_3$ (28 atoms).

The periodic model of a primitive $ZnSeO_3$ cell consisting of 28 atoms was used (Figure 6). The calculated lattice parameters (a, b, c), crystal density (ϱ_V) and effective charges of atoms (q_{eff}) are presented in Table 3 together with experimental results.

Table 3 – Calculated parameters of $ZnSeO_3$ crystal.

Parameter	Calculation	Experiment	Experiment [25]
a, Å	5.85	5.90	5.92
b, Å	7.69	7.64	7.66
c, Å	5.19	5.03	5.04
ρ_V (g/cm^3)	5.44	5.58	
q_{eff} (Zn/Se/O)	+1.16/+1.36/-0.84	-	

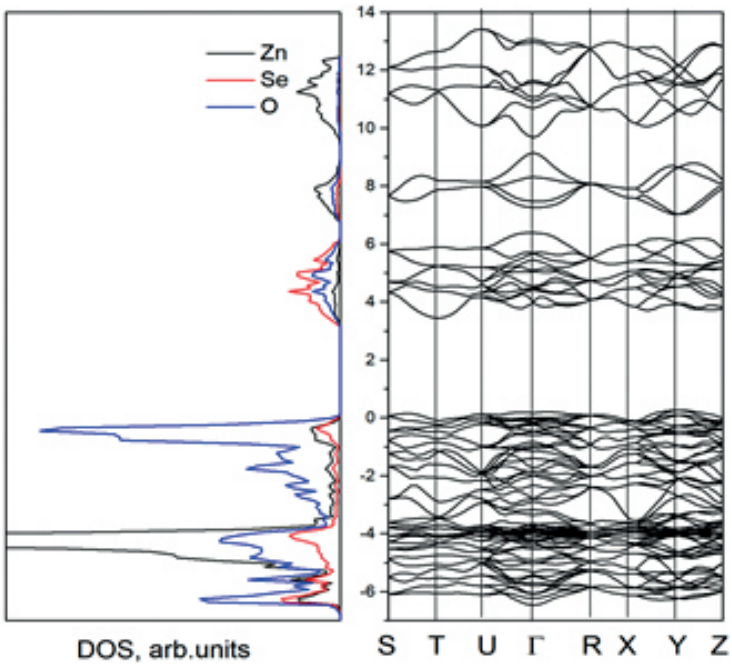

Figure 7 - Density of states and band structure of pure $ZnSeO_3$ crystal

Figure 7 shows the band structure at the highly symmetric Brillouin w points and along the directions between them, together with the density of electronic states. The valence band maximum appears near the Y-point, while the conduction band minimum occurs at the T-point, indicating the indirect band structure. The calculated width of the band gap is 3.8 eV. The density of electronic states shows that the top of the valence band is represented mainly by O 2p states, while the conduction band is mainly represented by Se 3d, 4s orbitals. The higher energy states are mainly represented by Zn 3d, 4s. As a result, it can be concluded that $ZnSeO_3$ has a typical ionic compound, although the charge distribution analysis showed a significant covalent contribution to the chemical bonds of the crystal.

5. Conclusions

$ZnSeO_3$ nanocrystals were synthesised, and their optical properties were investigated. The nanostructures were prepared by chemical deposition and electrochemical deposition into a track templated matrix. The crystal structure and phase composition were studied by XRD. The crystal phase of all samples was the same: orthorhombic structure, with almost identical unit cell parameters. The electrochemical deposition method was shown to be more optimal to create this crystal in comparison to the chemical deposition method. The use of electrochemical deposition method gives an opportunity to fill almost all the nanopores and hence it is more convenient and affordable method. The PL spectrum demonstrated a broad emission band in the spectrum interval of 2.2-3.3 eV. Non-empirical calculations of the $ZnSeO_3$ crystal were carried out, and the calculated band gap was 3.8 eV.

Acknowledgement

The article was performed as part of the implementation of the scientific project grant funding for young scientists under "Zhas Galym" project for 2022-2024 of the Science Committee of the Ministry of Science and Higher Education of the Republic of Kazakhstan AP13268607 "Features of the formation of semiconductor nanostructures in a track template SiO_2/Si"

References

1. Petrij O. A. Elektrosintez nanostruktur i nanomaterialov // Uspekh himii. – 2015. – V. 84. №2. –p. 159-193.

2. Kanyukov E.YU., Petrov A.V., Dem'yanov S.E., Ivanova YU.A., Ivanov D.K., Strel'cov E.A., Fedotov A.K., Fink D., Fahrner W.R.,, Fahrner W.R., Fizicheskie principy sozdaniya nanosensorov na osnove sistem Si/SiO2/metall s trekami bystryh tyazhelyh ionov // Sbornik dokladov mezhdunarodnoj konferencii «Aktual'nye problemy fiziki tverdogo tela», 2007 g., Minsk, Belarus', tom 2, s.384-388.

3. Fink D., Petrov A., Fahrner W.R., Hoppe H., Ulyashin A.G., Papaleo R.M., in: Proc. ISEC, Peking, China, 2003.

4. Fink D. (Ed.). Fundamentals of Ion-Irradiated Polymers // Springer Series in Materials Science. – 2004. – 406 p. doi:10.1007/978-3-662-07326-1

5. Petrov A.V., Fink D., Fahrner W.R., Hoppe K., Dem'yanov S.E., Fedotov A.K., Malyutina V.V.. // Sbornik dokladov «FTT-2005». Bronskaya. - 2005. - 482.

6. Dauletbekova A., Bajmuhanov Z., Kozlovskij A., Giniyatova Sh., Murzagaliev M., Zhurkin E., Nauryzbaeva R., Razrabotka i issledovanie nanokompozitnyh materialov na osnove trekovogo templejta SiO2/Si // Vestnik ENU. - 2018. №1(122). –p. 82-91.

7. Akylbekova A., Shayamanov B., Useinov A., Dauletbekova A., Bajmuhanov Z., Kozlovskij A., Giniyatova Sh., Popov A.I., Bajzhumanov M., Eksperimental'nye i teoreticheskie issledovaniya nanokristallov ZnSe2O5 // Vestnik ENU. – 2020. – V.130. №1. –p. 34-43.

8. Dauletbekova A., Akylbekova A., Giniyatova Sh., Bajmuhanov Z., Vlasukova L., Akilbekov A., Useinov A., Kozlovskij A., Karipbaev Zh., Struktura, elektricheskie svojstva i lyuminescenciya nanokristallov ZnO, elektroosazhdennyh v trekovye matricy SiO 2 /Si // Vestnik ENU. – 2019. №3 (128). –p. 57-66.

9. Akilbekov, A., Akylbekova A., Usseinov A., Kozlovskyi A., Baymukhanov Z., Giniyatova S., Dauletbekova, A. Ion track template technique for fabrication of ZnSe2O5 nanocrystals. Nuclear Instruments and Methods in Physics Research Section B: Beam Interactions with Materials and Atoms. – 2020. – Vol. 476. –P. 10–13. doi:10.1016/j.nimb.2020.04.039

10. Akylbekova A., Dauletbekova A., Baymukhanov Z., Kozlovsky A., Usseinov, A. Template synthesis of ZnSe2O5 nanocrystals // AIP Conf. Proc. – 2019. - V. 2174. –P. 020001. https://doi.org/10.1063/1.5134152

11. Dauletbekova A., Akylbekova A., Sarsekhan G., Usseinov A., Baimukhanov Z., Kozlovskiy A., Vlasukova L.A., Komarov, F.F., Popov A.I., Akilbekov A.T. Ion-Track Template Synthesis and Characterization of ZnSeO3 Nanocrystals // Crystals. – 2022. Vol. 12. –P. 817. https://doi.org/10.3390/cryst12060817

12. Kohn K., Inoue K., Horie O. et al. Crystal Chemistry of MSeO3 and MTeO3, (M = Mg, Mn, Co, Ni, Cu, and Zn) // J. Solid State Chemistry. – 1976. – Vol. 18, №1. – P. 27-37. https://doi.org/10.1016/0022-4596(76)90075-X

13. Ostanina T.N., Rudoi, V.M., Nikitin V.S., Darintseva A.B., Zalesova O.L., Porotnikova N.M. Determination of the surface of dendritic electrolytic zinc powders and evaluation of its fractal dimension // Russ. J. Non-Ferr. Met. - 2016. Vol. 57. – P. 47–51. doi: 10.3103/S1067821216010120

14. Studenikin S.A., Golego N., Cocivera M. Fabrication of green and orange photoluminescent, undoped ZnO films using spray pyrolysis // J. Appl. Phys. - 1998. Vol. 84. –P. 2287–2294. https://doi.org/10.1063/1.368295

15. Ashrafia A., Jagadish C. Review of zincblende ZnO: Stability of metastable ZnO phases // J. Appl. Phys. 2007. Vol. 102. –P. 071101. doi:10.1063/1.5143165

16. Degoda V.Y., Sofienko, A.O. Specific features of the luminescence and conductivity of zinc selenide on exposure to X-ray and optical excitation // Semiconductors. - 2010. Vol. 44. – P. 568–574. https://doi.org/10.1134/S1063782610050040

17. Degoda V.Y., Podust G.P., Doroshenko I.Y., Pavlova N.Y. Phosphorescence and conduction current relaxation in ZnSe crystals // Opt. Mater. - 2022. V. 129. –P. 112460. https://doi.org/10.1016/j.optmat.2022.112460

18. Kumano H., Ashrafi A.A., Ueta A. et al. Luminescence properties of ZnO films grown on GaAs substrates by molecular - beam epitaxy excited by electron – cyclotron resonance oxygen plasma // J. Crystal Growth. – 2000. – Vol. 214-215, №1-2. – P. 280-283. https://doi.org/10.1016/S0022-0248(00)00091-9

19. Perdew J.P., Zunger A. Self-interaction correction to density functional approximations for many-electron systems // Phys. Rev. B. – 1981. – Vol. 23. – P. 5048-5079.

20. Dirac P.A.M. Note on exchange phenomena in the Thomas-Fermi atom // Proc. Cambridge Phil. Soc. – 1930. – Vol. 26, №3. – P. 376-385.

21. Dovesi R., Saunders V.R., Roetti R. et al. CRYSTAL14: User's Manual. – Torino: University of Torino, 2016. – 382 p.

22. Jaffe J.E., Hess A.C. Hartree-Fock study of phase changes in ZnO at high pressure // Phys. Rev. B. – 1993. – Vol. 48, №11. – P. 7903-7909.

23. Towler M.D., Zicovich-Wilson C. Selenium basis set for the crystal program // https://vallico.net/mike_towler//basis_sets/Se_basis.txt. 4.04.2019.

24. Mulliken R. S. Electronic population analysis on LCAO-MO molecular wave functions // J. Chem. Phys. – 1955. – Vol. 23, №10. – P. 1833-1840.

25. Kohn K., Inoue K., Horie O. et al. Crystal Chemistry of MSeO3 and MTeO3, (M = Mg, Mn, Co, Ni, Cu, and Zn) // J. Solid State Chemistry. – 1976. – Vol. 18, №1. – P. 27-37.

Формирование нанокристаллов селенита цинка в трековых шаблонах SiO_2/Si с применением различных составов электролитов

А.Д. Акылбекова, Г.Г. Сарсехан, З.К. Баймуханов, А.К. Даулетбекова, Г.М. Аралбаева

Евразийский национальный университет им. Л.Н. Гумилева, Астана, Казахстан

Аннотация. В работе представлены исследования нанокристаллов селенита цинка, полученных химическим и электрохимическим осаждением цинка в трековом шаблоне диоксид кремния на кремний. С использованием двух типов электролитов были получены методом темплэйтного синтеза нанокристаллы селенита цинка и исследованы их морфологические, структурные и фотолюминесцентные свойства. Метод электрохимического осаждения оказался более эффективным для получения данного кристалла по сравнению с методом химического осаждения. Полученные нами параметры ячейки совпадают с литературными данными других работ. Спектры фотолюминесценции регистрировались в спектральном диапазоне от 2 до 4 эВ при комнатной температуре при длине волны возбуждения ~ 4 эВ.

Ключевые слова: диоксид кремния, химическое и электрохимическое осаждение, фотолюминесценция, нанокристаллы селенита цинка.

SiO_2/Si трек темплэйтінде электролиттердің екі түрін пайдалану негізінде мырыш селениті нанокристалдарының түзілуі

А.Д. Акылбекова, Г.Ғ. Сарсехан, З.К. Баймуханов, А.К. Даулетбекова, Г.М. Аралбаева

Л.Н. Гумилев атындағы Еуразия ұлттық университеті, Астана, Қазақстан

Аңдатпа. Мақалада a-SiO_2/Si-n трек темплэйтіндегі мырыштың химиялық және электрохимиялық тұндыруынан алынған мырыш селениті нанокристалдарының зерттеулері ұсынылды. Электролиттердің екі түрін қолдана отырып, мырыш селенитінің нанокристалдары шаблондық синтез арқылы алынды. Олардың морфологиялық, құрылымдық және фотолюминесценттік қасиеттері зерттелді. Бұл кристалды алу кезінде химиялық тұндыру әдісіне қарағанда электрохимиялық тұндыру әдісі тиімдірек болып шықты. Біз алған ұяшық параметрлері басқа еңбектердегі әдебиет деректерімен сәйкес келеді. Фотолюминесценция спектрлері ~ 4 эВ қозу толқын ұзындығындағы бөлме температурасында 2-ден 4 эВ-ге дейінгі спектрлік диапазонда жазылды.

Түйін сөздер: кремний диоксиді, химиялық және электрохимиялық тұндыру, фотолюминесценция, мырыш селенитінің нанокристалдары.